Available online at www.sciencedirect.com
SCIENCE DIRECT®
International Journal of Pharmaceutics 259 (2003) 115–127
international journal of pharmaceutics
www.elsevier.com/locate/ijpharm

Effect of copolymer composition on the physicochemical characteristics, in vitro stability, and biodistribution of PLGA–mPEG nanoparticles

K. Avgoustakis [a,*], A. Beletsi [a], Z. Panagi [a], P. Klepetsanis [a], E. Livaniou [b], G. Evangelatos [b], D.S. Ithakissios [a]

[a] *Pharmaceutical Technology Laboratory, Department of Pharmacy, University of Patras, Rion 26500, Patras, Greece*
[b] *Institute of Radioisotopes and Radiodiagnostic Products, NCSR "Demokritos", Aghia Paraskevi Attikis, Athens 15310, Greece*

Received 9 October 2002; received in revised form 3 March 2003; accepted 19 March 2003

Abstract

The physicochemical properties, the colloidal stability in vitro and the biodistribution properties in mice of different PLGA–mPEG nanoparticle compositions were investigated. The nanoparticles were prepared by a precipitation–solvent evaporation technique. The physical characteristics and the colloidal stability of the PLGA–mPEG nanoparticles were significantly influenced by the composition of the PLGA–mPEG copolymer used to prepare the nanoparticles. PLGA–mPEG nanoparticles prepared from copolymers having relatively high mPEG/PLGA ratios were smaller and less stable than those prepared from copolymers having relatively low mPEG/PLGA ratios. All PLGA–mPEG nanoparticle compositions exhibited prolonged residence in blood, compared to the conventional PLGA nanoparticles. The composition of the PLGA–mPEG copolymer affected significantly the blood residence time and the biodistribution of the PLGA–mPEG nanoparticles in liver, spleen and bones. The in vivo behavior of the different PLGA–mPEG nanoparticle compositions did not appear to correlate with their in vitro stability. Optimum mPEG/PLGA ratios appeared to exist leading to long blood circulation times of the PLGA–mPEG nanoparticles. This may be associated with the effects of the mPEG/PLGA ratio on the density of PEG on the surface of the nanoparticles and on the size of the nanoparticles.

Keywords: Poly(lactide-co-glycolide)-(polyethyleneglycol) nanoparticles; Biodistribution; Blood clearance; Copolymer composition; Colloidal stability

1. Introduction

Conventional polymeric nanoparticles are rapidly removed from bloodstream after intravenous (i.v.) administration by the macrophages of the mononuclear phagocyte system (MPS), mainly the Kupffer cells in the liver and the spleen macrophages. This prevents their application in controlled drug delivery and drug targeting to tissues other than MPS. Surface engineering, however, may lead to nanoparticles capable of evading, at least to some extent, MPS uptake which exhibit prolonged residence in blood. Thus, coating the nanoparticle surface with a hydrophilic polymer such as poly(ethylene glycol) (PEG) has been shown to confer long circulation properties to poly(lactide) (PLA), poly(lactide-co-glycolide) (PLGA), poly(caprolactone) (PCL) and poly(phosphazene) nanoparticles (Gref et al., 1994; Stolnik et al.,

* Corresponding author. Tel.: +30-2610-997726; fax: +30-2610-996302.
E-mail address: avgoust@upatras.gr (K. Avgoustakis).

0378-5173/03/$ – see front matter © 2003 Elsevier Science B.V. All rights reserved.
doi:10.1016/S0378-5173(03)00224-2

1994; Bazile et al., 1995; Dunn et al., 1997; Vandorpe et al., 1997). The presence of the hydrophilic coating on the surface of the nanoparticles is thought to sterically stabilize them against opsonization and phagocytocis. Between the hydrophilic polymers, PEG has been found to be a particularly effective steric stabilizer, probably due to its high hydrophilicity, chain flexibility, electrical neutrality and absence of functional groups, which prevent interactions with biological components in vivo (Gref et al., 1995). The stability of the PEG surface layer to desorption/displacement in vivo is essential for the long circulation effect (Gref et al., 1995; Neal et al., 1998). In this respect, PEG has been shown to be more effective when covalently bound on nanoparticle surface than when adsorbed in reducing complement activation and interaction of the nanoparticles with macrophages in vitro (Bazile et al., 1995; Vittaz et al., 1996; Mosqueira et al., 1999) as well as the uptake of nanoparticles by MPS in vivo (Mosqueira et al., 1999).

In recent years, PLA–PEG and PLA–PEG nanoparticles have extensively been investigated for their potential as controlled and targeted drug delivery systems. They are biocompatible and biodegradable (Gref et al., 1995), they exhibit prolonged blood circulation time after i.v. administration in experimental animals (Gref et al., 1994; Bazile et al., 1995; Verrecchia et al., 1995) and they can be stored as freeze-dried powders until use, provided that appropriate freeze-drying conditions are employed (De Jaeghere et al., 1999; Zambaux et al., 1999). Lipophilic drugs, proteins, neutral oligonucleotide complexes and plasmid DNA have successfully been incorporated in these nanoparticles (Gref et al., 1994; Emile et al., 1996; Peracchia et al., 1997; Tobio et al., 1998; Li et al., 2001; Perez et al., 2001; Vila et al., 2002). However, the incorporation efficiency of drugs with relatively high aqueous solubility in PLA–PEG and PLA–PEG nanoparticles is low (Govender et al., 2000; Redhead et al., 2001; Avgoustakis et al., 2002) and may require the development of more sophisticated incorporation techniques, such as the introduction of a drug complexation agent in the formulation (Govender et al., 2000), in order to be improved.

Riley et al. (1999) and Stolnik et al. (2001) have studied certain colloidal properties of micellar-like PLA–PEG nanoparticles. They reported that increasing the molecular weight of the PLA block resulted in significantly less colloidally stable nanoparticle dispersions. Nevertheless, the nanoparticles prepared from the copolymers with high molecular weight PLA blocks exhibited longer blood circulation times after i.v. administration in rats than the nanoparticles prepared from copolymers with low molecular weight PLA blocks (Stolnik et al., 2001). Mosqueira et al. (2001) prepared PEG-grafted nanocapsules using different PLA and PLA–PEG mixtures, so as to achieve different PEG contents in the nanocapsules, and studied their biodistribution properties. They concluded that long PEG chains and high PEG surface density are necessary to produce an increased half-life of the nanocapsules in vivo.

We have recently reported that within a dose range of approximately 100–1000 μg per mouse, conventional PLGA nanoparticles followed non-linear and dose-dependent pharmacokinetics whereas the PLGA–mPEG nanoparticles followed linear and dose-independent pharmacokinetics (Panagi et al., 2001). We have also shown that the i.v. administration of these PLGA–mPEG nanoparticles loaded with cisplatin in mice resulted in prolonged cisplatin residence in systemic blood circulation (Avgoustakis et al., 2002). In this communication, we present data on the effect of the PLGA–mPEG copolymer composition (PLGA/mPEG molar ratio) on the physicochemical properties, the in vitro stability and the tissue-distribution in mice of PLGA–mPEG nanoparticles. PLGA nanoparticles have also been included in the study for comparison purposes.

2. Materials and methods

2.1. Materials

DL-Lactide (LE) and glycolide (GE) were purchased from Boehringer Ingelheim (Germany). They were recrystallized twice from ethyl acetate and dried under high vacuum at room temperature before use. Monomethoxypoly(ethyleneglycol) (mPEG, molecular weight: 5000) was obtained from Sigma Chemical Co. (St. Louis, MO) and dried under high vacuum at room temperature before use. Stannous octoate, sodium cholate and cholesterylaniline (5-cholesten-3β-[*N*-phenyl]amine, CA) were also obtained from Sigma. Sepharose CL-4B gel was purchased from Pharmacia

(Sweden) and Biogel A15m from Bio-Rad. Tetrahydrofuran of HPLC grade and miscellaneous chemical reagents and solvents, all of analytical grade, were obtained from Sigma, Merck (Germany) and SDS (France). The $Na^{125}I$ was provided by NCSR "Demokritos" (Greece) (source: MDS Nordion, Belgium).

2.2. Synthesis and characterization of PLGA–mPEG copolymers

PLGA and PLGA–mPEG copolymers of different composition (PLGA/mPEG molar ratio) were prepared by a melt polymerization process under vacuum, using stannous octoate as catalyst (Beletsi et al., 1999). They were characterized with regard to their composition by ^{1}H-NMR and their molecular weight and molecular weight distribution (polydispersity index, P.I. = M_w/M_n) by gel permeation chromatography (GPC) (Beletsi et al., 1999). The following copolymers were synthesized: (1) PLGA with molar composition LA:GA = 2.8, $M_w = 22 \times 10^3$ and P.I. = 1.9; (2) PLGA–mPEG(495) with composition LA:GA:EO = 6.6:2.1:1.0, $M_w = 51 \times 10^3$ and P.I. = 3.2; (3) PLGA–mPEG(256) with composition LA:GA:EO = 3.5:1.0:1.0, $M_w = 27 \times 10^3$ and P.I. = 2.6; (4) PLGA–mPEG(153) with composition LA:GA:EO = 2.0:0.7:1.0, $M_w = 16 \times 10^3$ and P.I. = 2.6; (5) PLGA–mPEG(70) with composition LA:GA:EO = 0.9:0.3:1.0, $M_w = 14 \times 10^3$ and P.I. = 3.0; (6) PLGA–mPEG(61) with composition LA:GA:EO = 0.8:0.3:1.0, $M_w = 15 \times 10^3$ and P.I. = 2.2; and (7) PLGA–mPEG(34) with composition LA:GA:EO = 0.4:0.2:1.0, $M_w = 9 \times 10^3$ and P.I. = 2.1. LA, GA, and EO stand for lactic acid, glycolic acid, and ethyleneoxide components, respectively. The copolymers are referred to in the text as PLGA–mPEG(X), where X designates the molar ratio of (lactide+ glycolide)/mPEG in the copolymer, i.e. the PLGA/mPEG ratio, as determined by ^{1}H-NMR. The molecular weight and the P.I. of the mPEG used were measured by GPC to be $M_w = 5200$ and P.I. = 1.1, respectively.

2.3. Preparation of PLGA and PLGA–mPEG nanoparticles

PLGA and PLGA–mPEG nanoparticles were prepared using a precipitation–solvent evaporation technique (Panagi et al., 2001). Briefly, a solution of the polymer in acetone was transferred dropwise to a stirred aqueous solution of sodium cholate (12 mM). The mixture was kept under stirring until acetone had been evaporated, and the nanoparticle dispersion formed was condensed in a rotary evaporator (Buchi R114) and filtered through a 1.2-μm filter (Millex AP, Millipore).

The size and ζ-potential of the nanoparticles were determined using photon correlation spectroscopy (PCS) and microelectrophoresis, respectively, in a Malvern Z-sizer 5000 instrument (five runs per sample). The ζ-potential of the nanoparticles was measured in phosphate buffered saline (PBS), pH = 7.4. The surface area occupied by each PEG molecule on nanoparticle surface, S_{PEG} (nm^2 per molecule), i.e. the inverse density of PEG on nanoparticle surface, was determined as described by Bazile et al. (1995).

2.4. Study of the colloidal stability of the nanoparticles

The colloidal stability of the PLGA and PLGA–mPEG nanoparticles was evaluated from their resistance to electrolyte (Na_2SO_4 or $CaCl_2$)-induced nanoparticle aggregation and from the size stability of the nanoparticles during short-term storage at different conditions. In the study of nanoparticle stability in the presence of Na_2SO_4, the nanoparticles (125 μl) were added to 1 ml of sodium sulfate solutions of varying concentrations (0–1 M) incubated at 37 °C in a mildly shaking water bath. After 10 min, the turbidity of the dispersions was measured at 564 nm with a Shimadzu UV-1205 spectrophotometer. In the experiments with the $CaCl_2$, the nanoparticles (1 ml) were added to 2 ml of calcium chloride solutions of varying concentrations (0–30 mM Ca^{2+}) incubated at 37 °C in a mildly shaking water bath. After 5 min, the size of the dispersions was measured using PCS, as described in Section 2.3. In the study of nanoparticle stability during storage, the nanoparticles were incubated at 4 °C (refrigerator) or 37 °C (mildly shaking waterbath) for a period of 6 days. The size of the nanoparticles was determined every 24 h as described in Section 2.3.

2.5. Biodistribution study

PLGA and PLGA–mPEG nanoparticles labeled with ^{125}I-CA were prepared by the precipitation–

solvent evaporation technique, as we described in detail elsewhere (Panagi et al., 2001). The tissue distribution of the ^{125}I-CA label and the ^{125}I-CA-labeled PLGA and PLGA–mPEG nanoparticles was determined in female Swiss-De mice weighing 25–30 g. The animals, three per group, were injected at random in the tail vein with 100 μl nanoparticles (300 μg polymer per mouse) or 100 μl of a dispersion of the label in a water–ethanol (7:3 by volume) solvent (4.1 μCi). At predetermined time intervals, the mice were sacrificed, and their tissues (liver, spleen, lungs, muscle, bone (femur of left hind leg), intestines, kidney, urinary bladder, brain and thyroid) were excised, washed quickly with cold water to remove surface blood, and counted for radioactivity. Blood samples (0.07–0.08 g) were obtained in duplicate by cardiac puncture in pre-weighed heparinized tubes. The radioactivity remaining in the tail was also measured and taken into consideration in the calculation of total radioactivity dose administered to the animals. In the calculations of the %dose per organ, blood, bone and muscle were considered to constitute the 7, 10 and 43% of the body weight, respectively (Chiotelis et al., 1977). The biodistribution experiments adhered to the "Principles of Laboratory Animal Care" (NIH publication #85–23, revised 1985).

2.6. Statistical analysis of the data

Appropriate statistical procedures (*F*-test for means and Kruskal–Wallis test for medians, Statgraphics Plus 3.3 software) were applied for the statistical analysis of the experimental data.

3. Results

3.1. Physicochemical properties of the nanoparticles

The basic physicochemical characteristics of the nanoparticles are presented in Table 1. The PLGA nanoparticles were bigger and had a much lower ζ-potential than the PLGA–mPEG nanoparticles. Between the different PLGA–mPEG compositions, a clear trend of decreasing the size of the nanoparticles as their PEG content increased (i.e. as the PLGA/mPEG molar ratio decreased) was observed. Also, the density of PEG on nanoparticle surface increased when the PEG content of nanoparticles was increased, as evidenced by the decrease of the S_{PEG} values when the PLGA/mPEG ratio fell.

3.2. Colloidal stability of the nanoparticles

The turbidity of nanoparticles of different composition in the presence of increasing concentrations of Na_2SO_4 is shown in Fig. 1. A significant increase in turbidity signified the onset of nanoparticle flocculation, and the concentration of Na_2SO_4 at which flocculation occurred depended on nanoparticle composition. The PLGA–mPEG(495) and PLGA–mPEG(256) nanoparticles, which have relatively low PEG content (high PLGA/mPEG ratio) were less resistant to Na_2SO_4-induced aggregation than the PLGA–mPEG(70) and PLGA–mPEG(34) nanoparticles, which have relatively high PEG content (low PLGA/mPEG ratio). The PLGA nanoparticles appeared to have similar stability in the presence of Na_2SO_4 with the PLGA–mPEG nanoparticles

Table 1
Physicochemical characteristics and biological performance (%dose remaining in blood 3 h after i.v. injection in mice) of the nanoparticle compositions involved in the present study

Composition	Size (nm)	Size polydispersity	ζ-potential (mV)	S_{PEG} (nm^2 per molecule)	%dose in blood (3 h)
PLGA	133.5 ± 20.1	0.489	−54.2	–	4.1
PLGA–mPEG(495)	114.8 ± 11.1	0.245	−6.2	2.8	34.4
PLGA–mPEG(256)	97.4 ± 3.5	0.385	−5.9	2.0	42.6
PLGA–mPEG(153)	79.0 ± 14.2	0.245	−4.7	1.7	63.9
PLGA–mPEG(70)	69.6 ± 10.8	0.356	−5.9	1.4	54.9
PLGA–mPEG(61)	67.0 ± 6.6	0.292	−5.2	1.4	48.9
PLGA–mPEG(34)	57.5 ± 17.3	0.347	−4.3	1.3	31.6

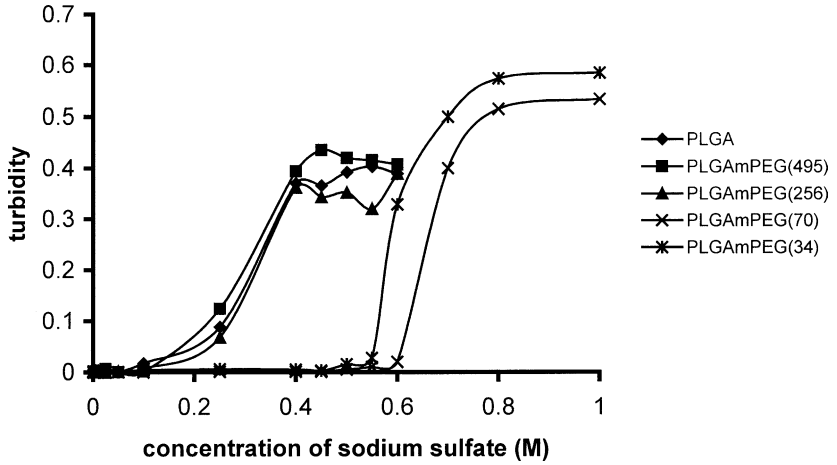

Fig. 1. Effect of sodium sulfate concentration on the turbidity of PLGA and PLGA–mPEG nanoparticles.

having relatively low PEG content, although their turbidity started to show a noticeable increase at a lower Na_2SO_4 concentration than the PLGA–mPEG nanoparticles (0.1 versus 0.25 M Na_2SO_4, respectively). Taking that the critical flocculation point (CFPT) is the electrolyte concentration at which a dramatic increase in the turbidity was first observed [23], the CFPT (M Na_2SO_4) for the nanoparticle compositions tested may be considered to be as follows: for the PLGA, PLGA–mPEG(495), and PLGA–mPEG (256) 0.25; for the PLGA–mPEG(34) 0.6; and for the PLGA–mPEG(70) 0.7 (Fig. 1).

The effect of the presence of increasing amounts of $CaCl_2$ in the nanoparticle dispersion on the size of the nanoparticles is shown in Fig. 2. The PLGA nanoparticles were clearly less resistant to the $CaCl_2$-induced flocculation than the PLGA–mPEG nanoparticles. They exhibited a dramatic increase (approximately

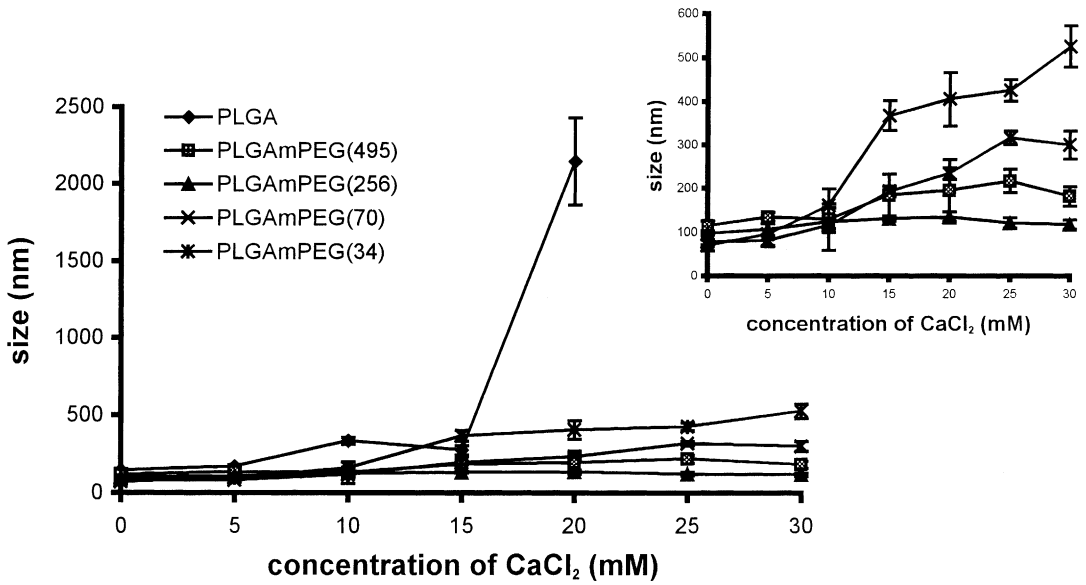

Fig. 2. Effect of calcium chloride concentration on the size of PLGA and PLGA–mPEG nanoparticles.

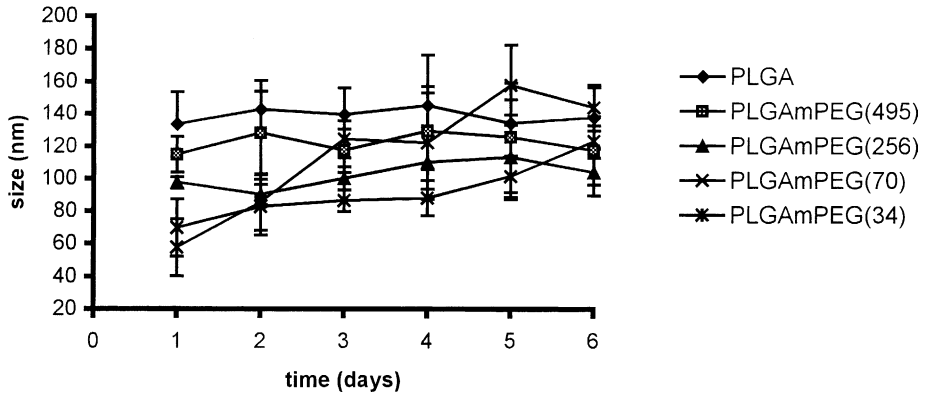

Fig. 3. Variation of the size of PLGA and PLGA–mPEG nanoparticles with incubation time at 37 °C.

15-fold) of their size at a concentration of 20 mM $CaCl_2$. The PLGA–mPEG(495) and PLGA–mPEG (256) nanoparticles, which have relatively low PEG content, appeared to be more resistant to $CaCl_2$-induced flocculation (i.e. they exhibited a lower size variation as the concentration of $CaCl_2$ increased) than the PLGA–mPEG(70) and PLGA–mPEG(34) nanoparticles, which have relatively high PEG content (inset in Fig. 2, in which the curves of the PLGA–mPEG nanoparticles only have been reproduced, facilitating their comparison).

The variation of the size of nanoparticles of different composition with incubation time at 37 °C is shown in Fig. 3. The size of the PLGA and the PLGA–mPEG nanoparticles having relatively low PEG content did not change significantly with time, whereas the size of the PLGA–mPEG nanoparticles having relatively high PEG content increased significantly with time. At the end of the incubation period, the size of the different nanoparticles had undergone the following percent change: PLGA 3.0%, PLGA–mPEG(495) 2.4%, PLGA–mPEG(256) 2.7%, PLGA–mPEG(70) 96.5% ($P < 0.05$), and PLGA–mPEG(34) 150.1% ($P < 0.05$). At 4 °C, the size of all nanoparticle compositions did not change significantly with time during the incubation period studied (data not shown).

3.3. Biodistribution of the free label and labeled nanoparticles

The tissue distribution of ^{125}I-CA and ^{125}I-CA-labeled PLGA–mPEG(61) and PLGA nanoparticles for a 24-h period post-administration is shown in Fig. 4. Initially, i.e. at 2 min post-injection (first sampling point), the major part of radioactivity was found in liver and muscles (43.8 and 35.2%, respectively) in the case of the free label, in blood (75.8%) in the case of the PLGA–mPEG nanoparticles, and in liver (70.9%) in the case of PLGA nanoparticles. After the first 2 min, the major tissue (re)distribution of radioactivity in the case of the free label appeared to be the gradual removal of radioactivity from muscles with time and its accumulation in the liver or its excretion in intestines and urine: the amount of radioactivity in other tissues changed little during the 2-min to 24-h period studied. The %dose of radioactivity in blood 2 min post-administration of the free label was 6.6. In the case of the PLGA–mPEG nanoparticles, the major radioactivity tissue (re)distribution process that took place after the first 2 min involved the slow removal of radioactivity from blood with time and its accumulation mainly in MPS tissues, such as liver and spleen, whereas in the case of the PLGA nanoparticles, the radioactivity was gradually removed from liver and excreted in intestines and urine during the same period of time. Following the administration of the labeled PLGA–mPEG nanoparticles, the radioactivity %dose in blood fell gradually with time from 75.8 at 2 min to 6.8 at 24 h. After the administration of the labeled PLGA nanoparticles, the %dose of radioactivity measured in blood was 4.9 at 2 min, then fell slightly with time to become 3.1% at 1 h, and then increased a little with time to reach 6.4 at 24 h (Fig. 4). The PLGA nanoparticles exhibited higher accumulation

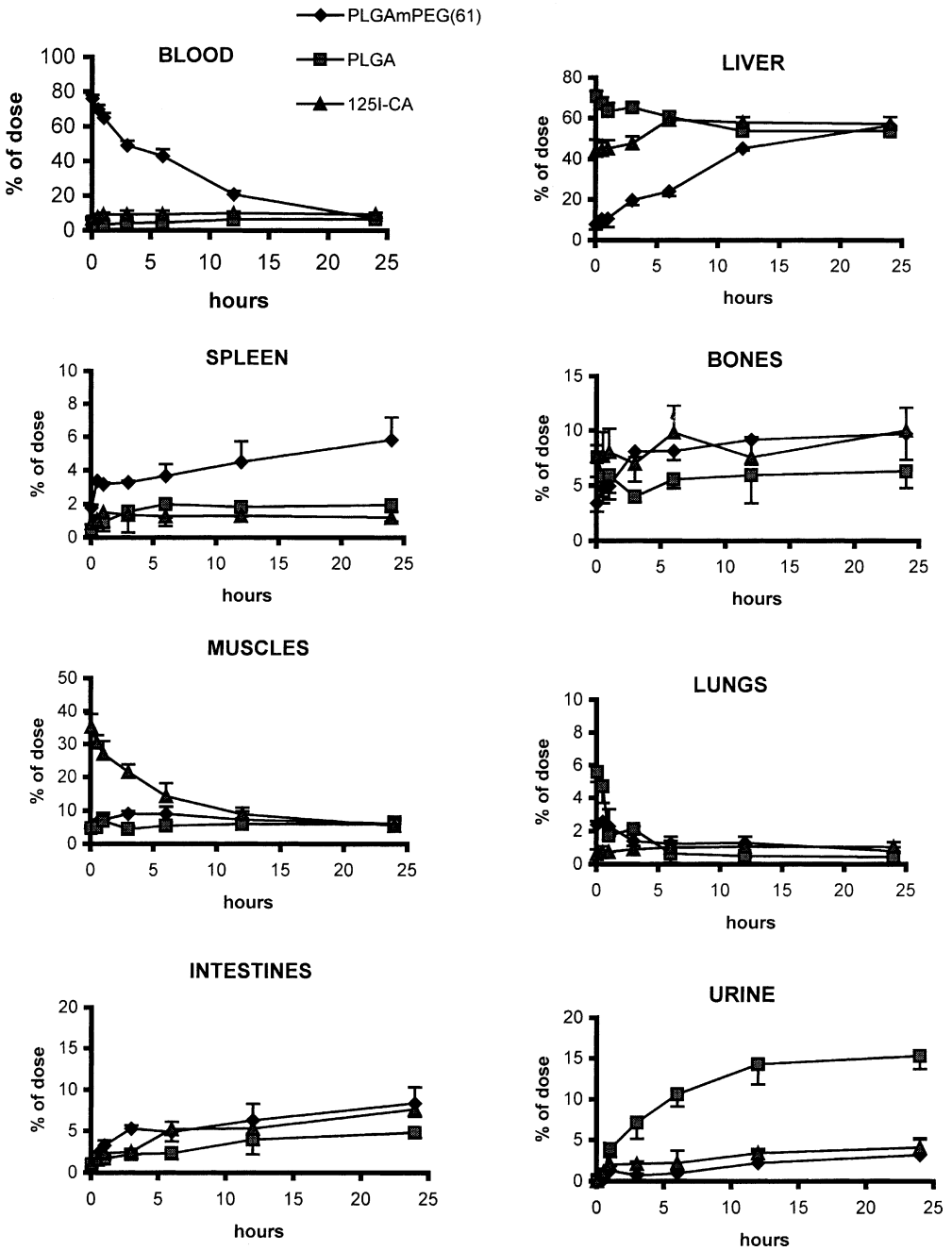

Fig. 4. Biodistribution of radioactivity with time following the i.v. administration of ^{125}I-CA and ^{125}I-CA-labeled PLGA and PLGA–mPEG(61) nanoparticles in mice.

in the lungs than the PLGA–mPEG nanoparticles at the early post-administration times (Fig. 4), possibly due to their higher size. The free label did not have any tendency to accumulate in the lungs as its %dose in the lungs never exceeded the 1% (Fig. 4).

3.4. Biodistribution of PLGA–mPEG nanoparticles of different composition

The variation of radioactivity %dose with time in blood after the i.v. administration of labeled PLGA–mPEG nanoparticles having different composition (PLGA/mPEG ratio) is shown in Fig. 5. With all compositions, the radioactivity exhibited prolonged blood residence. However, the rate of radioactivity removal from blood was significantly different for the different nanoparticle compositions. An increase in the PEG content of the PLGA–mPEG nanoparticles (i.e. a decrease of the PLGA/mPEG ratio from 256 to 153) caused initially a decrease in the rate of radioactivity clearance, which reached a minimum at a PLGA/mPEG ratio of 153, but then, a further increase in the PEG content of nanoparticles (i.e. a further decrease of the PLGA/mPEG ratio from 153 to 61 and then to 34) caused an increase in the rate of radioactivity blood clearance. The effect of copolymer composition on the in vivo blood longevity of the PLGA–mPEG nanoparticles for a wider range of compositions can also be seen in Table 1, where the %dose of the injected nanoparticles remaining in the systemic blood circulation 3 h post-administration is given for nanoparticles with PLGA/mPEG molar ratios between 495 and 34. The blood longevity of the nanoparticles increased with an initial decrease of the PLGA/mPEG ratio (in the range of ratios between 495 and 153) but decreased with a further decrease of the PLGA/mPEG ratio (in the range between 153 and 34).

With all nanoparticle compositions, the radioactivity levels in the liver increased with time (Fig. 5). The effect of nanoparticle composition in the capture of the PLGA–mPEG nanoparticles in the liver was the reverse of that observed in the blood: the nanoparticle compositions exhibiting high rate of blood clearance exhibited low rate of accumulation in liver and vice versa (Fig. 5). The radioactivity levels in the spleen increased slowly with time and reached 2–5% of the dose 6 h post-administration

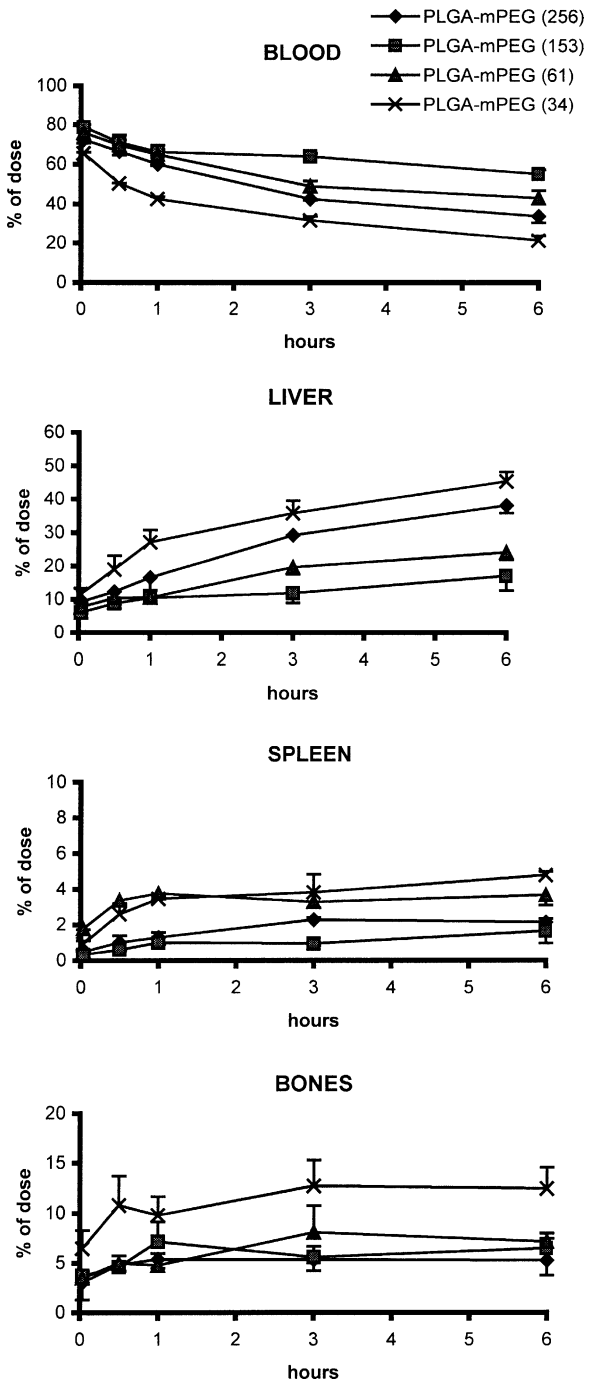

Fig. 5. Biodistribution of radioactivity with time in blood, liver, spleen and bones following the i.v. administration of ^{125}I-CA-labeled PLGA–mPEG nanoparticles of different composition in mice.

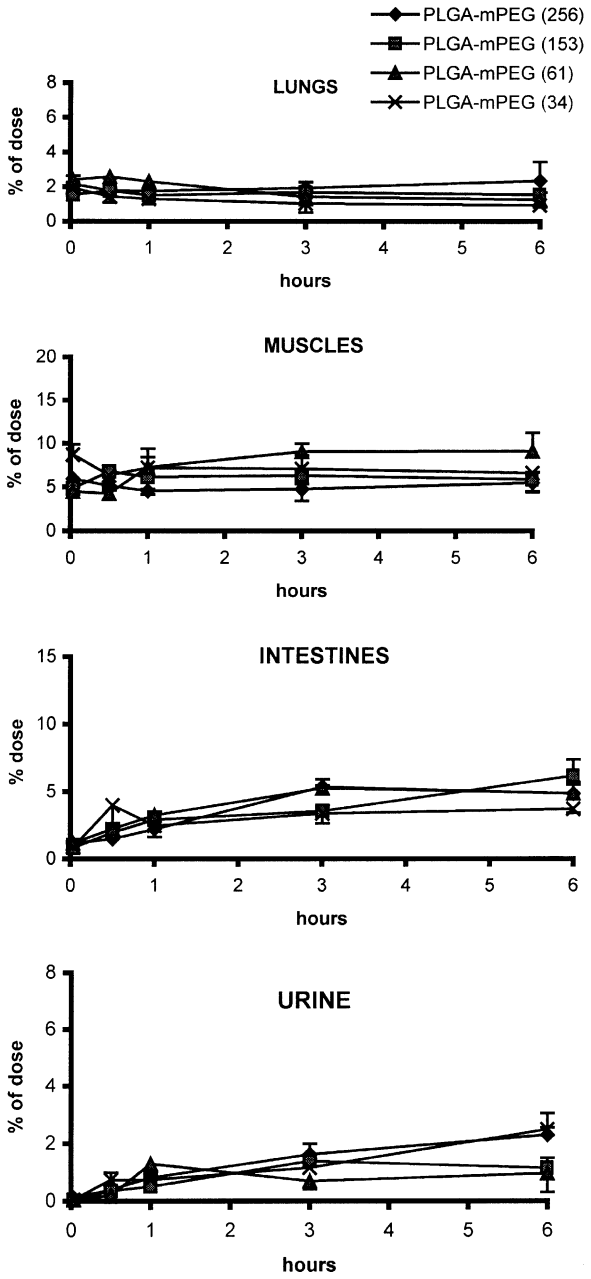

Fig. 6. Biodistribution of radioactivity with time in lungs, muscles, intestines and urine following the i.v. administration of ^{125}I-CA-labeled PLGA–mPEG nanoparticles of different composition in mice.

with the different nanoparticle compositions (Fig. 5). The PLGA–mPEG(34) nanoparticles exhibited significantly ($P < 0.05$) higher accumulation in the bones (12.5% of the injected dose) than the other nanoparticle compositions (5–8% of the dose) at the end of the 6-h period studied (Fig. 5).

The radioactivity dose accumulated in the muscles did not differ between the different nanoparticle compositions and was lower than 10% for all of them at the end of the 6-h period (Fig. 6). With all nanoparticle compositions, low levels of radioactivity were found in the lungs (1–2.5% of dose) (Fig. 6). With all nanoparticle compositions, the amount of radioactivity excreted in intestines and urine increased slowly with time, to reach a total level of 6–8% at the end of the sampling period (Fig. 6). No significant difference in the excretion rate could be observed between the different nanoparticle compositions. With all nanoparticle compositions, the radioactivity levels in other tissues not included in Figs. 5 and 6 were very low at all times post-administration. For example, the %dose of radioactivity measured in kidneys was 0.8–1.9%, in stomach 0.4–0.9%, in brain 0.1–0.5% and in thyroid 0.1–0.3% of the injected dose.

4. Discussion

In this work, the physicochemical properties, the in vitro stability and the biodistribution properties of PLGA–mPEG nanoparticles having different composition (PLGA/mPEG ratio) were investigated. Conventional PLGA nanoparticles were also included in this study for comparison reasons. The PLGA–mPEG nanoparticles had ζ-potential values relatively close to neutral due to the presence of PEG on their surface which covers the surface charges, whereas the PLGA nanoparticles had a highly negative ζ-potential. Also, the PLGA–mPEG nanoparticles were smaller than the PLGA nanoparticles and their size decreased as their PEG content (mPEG/PLGA ratio) increased (Table 1). The latter would indicate that PEG is able to moderate the association of the copolymer molecules during the formation of the particles and may be considered to be an indirect evidence of the micellar-like structure of the PLGA–mPEG nanoparticles prepared in this study (Riley et al., 1999).

The colloidal stability of the nanoparticles was first evaluated by their resistance to aggregation in the presence of electrolytes. The nanoparticle compositions with relatively high PEG content, such as the PLGA–mPEG(70) and PLGA–mPEG(34) nanoparticles, were more stable than the nanoparticle compositions with relatively low PEG content, such as the PLGA–mPEG(495) and PLGA–mPEG(256) nanoparticles, in the presence of increasing concentrations of sodium sulfate (Fig. 1). The lower stability of the nanoparticles with relatively low PEG content in the presence of sodium sulfate may be attributed to the incomplete coverage of nanoparticle surface by the PEG chains. Under the stress generated by Brownian collisions, the PEG chains are unable to prevent close approach of the nanoparticles. Then, when the surface charge of the nanoparticles is neutralized by the electrolyte, the van der Waals attraction between the PLGA cores leads to nanoparticle flocculation. The flocculation of the nanoparticles having relatively high PEG content at high sodium sulfate concentrations may be attributed to the decreased solvency power of water for PEG at these high concentrations of SO_4^{2-}. At sodium sulfate concentrations exceeding the θ point for the PEG, the PEG chains become dehydrated, the interaction between the PEG chains becomes attractive, and nanoparticle flocculation occurs (Riley et al., 1999).

In contrast to the results obtained with sodium sulfate, the PLGA–mPEG(495) and PLGA–mPEG(256) nanoparticles, which have relatively low PEG content, appeared to be more resistant to $CaCl_2$-induced flocculation (i.e. they exhibited a lower size variation as the concentration of $CaCl_2$ increased) than the PLGA–mPEG(70) and PLGA–mPEG(34) nanoparticles, which have relatively high PEG content (Fig. 2). The same result was obtained when the nanoparticles were incubated at 37 °C during a period of 6 days (Fig. 3). Based on NMR data, Stolnik et al. (2001) suggested that the nanoparticles prepared from PLA–PEG copolymers with low molecular weight PLA blocks (i.e. nanoparticles with high PEG content) are in a less solid state than the nanoparticles prepared from PLA–PEG copolymers having high molecular weight PLA blocks. Thus, the lower stability of the PLGA–mPEG nanoparticles with relatively high PEG content in the presence of $CaCl_2$ and upon incubation at 37 °C observed in the present study may be related to the lower rigidity of the cores of these particles and to the higher mobility of their chains, which would probably facilitate their aggregation in the presence of Ca^{2+} or with incubation time.

We have observed that the nanoparticles with high PEG content undergo significant degradation during the first 7 days of incubation at 37 °C in vitro (they loose approximately 50–70% of their mass, depending on their composition) (Avgoustakis et al., 2002). The higher degradation of the nanoparticles with relatively high PEG content may also contribute to their reduced stability (increased aggregation during storage) compared to the nanoparticles with relatively low PEG content, which exhibit lower degradation. When the nanoparticles were incubated at 4 °C under no agitation, both the collisions and the degradation of the nanoparticles were probably slowed down, and all nanoparticle compositions appeared to be equally stable (no aggregation occurred) during the period of 6 days investigated.

In order to investigate the biodistribution properties of the PLGA and PLGA–mPEG nanoparticles, the nanoparticles were labeled with ^{125}I-CA. The free ^{125}I-CA had completely different biodistribution properties than the ^{125}I-CA-labeled nanoparticles (Fig. 4). For example, it was rapidly removed from the blood pool, falling to less than 7% of the dose 2 min post-injection. Also, it exhibited a high accumulation in the muscle tissue (35.2% of dose at 2 min post-injection). On the contrary, the ^{125}I-CA-labeled PLGA–mPEG nanoparticles were slowly removed from blood, reaching the low radioactivity levels that the free label reached within 2 min at 24 h post-administration, and did not have the tendency to accumulate in muscles (the %dose measured in muscles 2 min post-administration was 4.5%). Furthermore, in the case of the PLGA–mPEG nanoparticles, the radioactivity levels in spleen increased slowly with time during the whole period tested, starting from 1.7% at 2 min and reaching 5.9% at 24 h. On the contrary, in the case of the free label, the radioactivity in the spleen did not change with time, being around 1% at all times post-administration. These results would indicate that the label was still associated with the PLGA–mPEG nanoparticles during the 24-h period tested and that these nanoparticles were slowly captured by spleen macrophages during this period. Also, the radioactivity measured in the

thyroid tissue was very low (lower than 0.3% of the dose) during the 24 h investigated, indicating that ^{125}I was not liberated from the ^{125}I-CA label during that period. Finally, in vitro studies demonstrated that about 80% of the label remained associated with the nanoparticles after 6-h incubation of ^{125}I-CA-labeled PLGA–mPEG nanoparticles in serum (Panagi et al., 2001). Therefore, ^{125}I-CA was considered to be a suitable label in order to follow the tissue distribution properties of the different PLGA–mPEG nanoparticle compositions during a period of 6 h, which was the major objective of our in vivo study.

All PLGA–mPEG nanoparticle compositions exhibited prolonged residence in blood, compared to the conventional PLGA nanoparticles (Table 1 and Figs. 4 and 5). The major pathway for the removal of all PLGA–mPEG compositions from blood appeared to be the nanoparticle capture in MPS tissues, and especially in the liver (Fig. 5). Comparatively, little radioactivity (6–8% of dose) was excreted in urine and intestines during the 6-h period investigated, and the radioactivity did not appear to accumulate in any other tissue during that period (Fig. 6). A composition effect on the blood clearance rate of PLGA–mPEG nanoparticles is clearly evident (Fig. 5). An increase in the PEG content of the PLGA–mPEG nanoparticles (i.e. a decrease of the PLGA/mPEG ratio) caused initially a decrease in the rate of nanoparticle clearance, but a further increase in the PEG content of nanoparticles caused an increase in the rate of nanoparticle clearance from blood. This result may be attributed to the effect the composition of the nanoparticles has on the PEG density on nanoparticle surface and the size of the nanoparticles. An increase in the PEG content of the nanoparticles, from composition PLGA–mPEG(256) to composition PLGA–mPEG(153), causes initially an increase in the PEG density on nanoparticle surface (Table 1, S_{PEG} values) and a more effective steric barrier is formed on nanoparticle surface, inhibiting nanoparticle opsonization and phagocytocis. As a result, the blood circulation time of the PLGA–mPEG(153) nanoparticles was higher than that of PLGA–mPEG(256) nanoparticles (Fig. 5). With a further increase in the PEG content of nanoparticles, compositions PLGA–mPEG(61) and PLGA–mPEG(34), PEG may still form an effective steric barrier on nanoparticle surface, the size however of the nanoparticles has now become sufficiently low to permit the nanoparticles to reach tissues that the bigger nanoparticles cannot. As it can be seen in Table 1, the size of PLGA–mPEG(61) and PLGA–mPEG(34) nanoparticles is lower than 70 nm. As a result, the blood circulation time of PLGA–mPEG(61) and especially PLGA–mPEG(34) nanoparticles was lower than that of PLGA–mPEG(153) nanoparticles (Fig. 5). It may be possible that these relatively small nanoparticles can penetrate more efficiently than the bigger nanoparticles through the fenestrae in the endothelial lining of the liver and associate with parenchymal cells. This would explain the increased liver accumulation of the PLGA–mPEG(61) and PLGA–mPEG(34) nanoparticles compared to the PLGA–mPEG(153) nanoparticles, which are bigger (Table 1). Stolnik et al. (2001) reported that their preliminary results suggest that small sterically stabilized particles can distribute mainly to the parenchymal cells of the liver after i.v. injection.

Further, evidence that the small PLGA–mPEG nanoparticles are more highly distributed in the body may be considered to provide the higher accumulation of the PLGA–mPEG(34) nanoparticles in bones (Fig. 5). PLGA–mPEG(34) nanoparticles had the smallest size (57.5 nm) of all nanoparticle compositions investigated (Table 1). The higher accumulation of these nanoparticles in bone marrow may be the result of their small size. The major part of the radioactivity measured in the bones is considered to result form nanoparticle capture in phagocytic reticuloendothelial cells lining the vascular sinusoids of bone marrow. However, this has to be demonstrated with appropriate tissue fractionation experiments. No significant differences between the different PLGA–mPEG nanoparticle compositions were observed in the accumulation of the nanoparticles in the other animal tissues (Fig. 6).

With the exception of the PLGA–mPEG(61) nanoparticles, the effect of the nanoparticle composition on the tendency of the PLGA–mPEG nanoparticles to accumulate in the spleen was similar to the effect the nanoparticle composition had on nanoparticle tendency to accumulate in the liver: the compositions exhibiting low liver accumulation also exhibited low spleen accumulation and vice versa (Fig. 5). It should also be noted that the PLGA–mPEG nanoparticles exhibited higher accumulation in the spleen than the

PLGA nanoparticles (Fig. 4), possibly due to their reduced sequestration by the liver.

A comparison of the in vitro stability data (Figs. 1–3) and the biodistribution data (Figs. 5 and 6) obtained with the different PLGA–mPEG nanoparticle compositions, reveal that the behavior of the PLGA–mPEG nanoparticles in vivo does not correlate with their colloidal stability in vitro (irrespective of the type of the in vitro experiment used to evaluate the stability of the nanoparticles). For example, the PLGA–mPEG(34) nanoparticles had significantly higher CFPT in the presence of sodium sulfate than the PLGA–mPEG(495) and the PLGA–mPEG(256) nanoparticles (Fig. 1) but lower longevity in blood (Fig. 5). Also, the PLGA–mPEG(70) nanoparticles were less stable in the presence of calcium chloride than the PLGA–mPEG(256) and PLGA–mPEG(495) nanoparticles (Fig. 2) but had higher blood longevity than them (Table 1).

5. Conclusions

The physical characteristics and the colloidal stability in vitro of the PLGA–mPEG nanoparticles were significantly influenced by the composition of the PLGA–mPEG copolymer used to prepare the nanoparticles. PLGA–mPEG nanoparticles prepared from the copolymers having relatively high mPEG/PLGA ratios were smaller and less stable than those prepared from PLGA–mPEG copolymers having relatively low mPEG/PLGA ratios. The in vivo behavior of the different PLGA–mPEG nanoparticle compositions did not appear to correlate with their in vitro stability. The composition of the PLGA–mPEG copolymer affected significantly the blood residence time and the biodistribution of the PLGA–mPEG nanoparticles in liver, spleen and bones. No significant differences between the different nanoparticle compositions were observed in the accumulation of the nanoparticles in the other tissues examined. Optimum mPEG/PLGA ratios appeared to exist leading to long blood circulation times of the PLGA–mPEG nanoparticles. This may be associated with the effects of the mPEG/PLGA ratio on the density of PEG on the surface of the nanoparticles and on the size of the nanoparticles.

References

Avgoustakis, K., Beletsi, A., Panagi, Z., Klepetsanis, P., Karydas, A.G., Ithakissios, D.S., 2002. PLGA–mPEG nanoparticles of cisplatin: in vitro nanoparticle degradation, in vitro drug release and in vivo drug residence in blood properties. J. Control Release 79, 123–135.

Bazile, D., Prud'Homme, C., Bassoullet, M.T., Marlard, M., Spenlehauer, G., Veillard, M., 1995. Stealth Me.PEG-PLA nanoparticles avoid uptake by the mononuclear phagocytes system. J. Pharm. Sci. 84, 493–498.

Beletsi, A., Leondiadis, L., Klepetsanis, P., Ithakissios, D.S., Avgoustakis, K., 1999. Effect of preparative variables on the properties of PLGA–mPEG copolymers related to their application in controlled drug delivery. Int. J. Pharm. 182, 187–197.

Chiotelis, E., Subramanian, G., McAfee, J.G., 1977. Preparation of Tc-99m labeled pyridoxal-amino acid complexes and their evaluation. Int. J. Nucl. Med. Biol. 4, 29–41.

De Jaeghere, F., Allemann, E., Leroux, J.C., Stevels, W., Feijen, J., Doelker, E., Gurny, R., 1999. Formulation and lyoprotection of poly(lactic acid-co-ethylene oxide) nanoparticles: influence on physical stability and in vitro cell uptake. Pharm. Res. 16, 859–866.

Dunn, S.E., Coombes, A.G.A., Garnett, M.C., Davis, S.S., Davies, M.C., Illum, L., 1997. In vitro cell interaction and in vivo biodistribution of poly(lactide-co-glycolide) nanospheres surface modified by poloxamer and poloxamine copolymers. J. Control Release 44, 65–76.

Emile, C., Bazile, D., Herman, F., Helene, C., Veillard, M., 1996. Encapsulation of oligonucleotides in Stealth Me.PEG-PLA_{50} nanoparticles by complexation with structured oligopeptides. Drug Deliv. 3, 187–195.

Govender, T., Riley, T., Ehtezazi, T., Garnett, M.C., Stolnik, S., Illum, L., Davis, S.S., 2000. Defining the drug incorporation properties of PLA–PEG nanoparticles. Int. J. Pharm. 199, 95–110.

Gref, R., Minamitake, Y., Peracchia, M.T., Trubetskoy, V., Torchilin, V., Langer, R., 1994. Biodegradable long-circulating polymeric nanospheres. Science 263, 1600–1603.

Gref, R., Domb, A., Quellec, P., Blunk, T., Muller, R.H., Verbavatz, J.M., Langer, R., 1995. The controlled intravenous delivery of drugs using PEG-coated sterically stabilized nanospheres. Adv. Drug Deliv. Rev. 16, 215–223.

Li, Y., Zhang, X., Gu, Z., Zhou, Z., Yuan, W., Zhou, J., Zhu, J., Gao, X., 2001. PEGylated PLGA nanoparticles as protein carriers: synthesis, preparation and biodistribution in rats. J. Control Release 71, 203–211.

Mosqueira, V.C.F., Lengrand, P., Gref, R., Heurtault, B., Appel, M., Barratt, G., 1999. Interactions between a macrophage cell line (J774A1) and surface-modified poly(D,L-lactide) nanocapsules bearing poly(ethylene glycol). J. Drug Target. 7, 65–78.

Mosqueira, V.C.F., Lengrand, P., Morgat, J.-L., Vert, M., Mysiakine, E., Gref, R., Devissaguet, J.-P., Barratt, G., 2001. Bodistribution of long-circulating PEG-grafted nanocapsules in mice: effects of PEG chain length and density. Pharm. Res. 18, 1411–1419.

Neal, J.C., Stolnik, S., Garnett, M.C., Davis, S.S., Illum, L., 1998. Modification of the copolymers poloxamer 407 and poloxamine 908 can affect the physical and biological properties of surface modified nanospheres. Pharm. Res. 15, 318–324.

Panagi, Z., Beletsi, A., Evangelatos, G., Livaniou, E., Ithakissios, D.S., Avgoustakis, K., 2001. Effect of dose on the biodistribution and pharmacokinetics of PLGA and PLGA–mPEG nanoparticles. Int. J. Pharm. 221, 143–152.

Peracchia, M.T., Gref, R., Minamitake, Y., Domb, A., Lotan, N., Langer, R., 1997. PEG-coated nanospheres from amphiphilic diblock and multiblock copolymers: investigation of their drug encapsulation and release characteristics. J. Control Release 46, 223–231.

Perez, C., Sanchez, A., Putnam, D., Ting, D., Langer, R., Alonso, M.J., 2001. Poly(lactic acid)-poly(ethylene glycol) nanoparticles as new carriers for the delivery of plasmid DNA. J. Control Release 75, 211–224.

Redhead, H.M., Davis, S.S., Illum, L., 2001. Drug delivery in poly(lactide-co-glycolide) nanoparticles surface modified with poloxamer 407 and poloxamine 908: in vitro characterization and in vivo evaluation. J. Control Release 70, 353–363.

Riley, T., Govender, T., Stolnik, S., Xiong, C.D., Garnett, M.C., Illum, L., Davis, S.S., 1999. Colloidal stability and drug incorporation aspects of micellar-like PLA–PEG nanoparticles. Colloids Surfaces B: Biointerfaces 16, 147–159.

Stolnik, S., Dunn, S.E., Garnett, M.C., Davies, M.C., Coombes, A.G.A., Taylor, D.C., Irving, M.P., Purkiss, S.C., Tadros, T.F., Davis, S.S., Illum, L., 1994. Surface modification of poly(lactide-co-glycolide) nanospheres by biodegradable poly(lactide)-poly(ethyleneglycol) copolymers. Pharm. Res. 11, 1800–1808.

Stolnik, S., Heald, C.R., Neal, J., Garnett, M.C., Davis, S.S., Illum, L., Purkis, S.C., Barlow, R.J., Gellert, P.R., 2001. Polylactide-poly(ethylene glycol) micellar-like particles as potential drug carriers: production, colloidal properties and biological performance. J. Drug Target 9, 361–378.

Tobio, M., Gref, R., Sanchez, A., Langer, R., Alonso, M.J., 1998. Stealth PLA–PEG nanoparticles as protein carriers for nasal administration. Pharm. Res. 15, 270–275.

Vandorpe, J., Schacht, E., Dunn, S., Hawley, A., Stolnik, S., Davis, S.S., Garnett, M.C., Davies, M.C., Illum, L., 1997. Long circulating biodegradable polyphosphazene nanoparticles surface modified with polyphosphazene-poly(ethylene oxide) copolymer. Biomaterials 18, 1147–1152.

Verrecchia, T., Spenlehauer, G., Bazile, D.V., Murry-Brelier, A., Archimbaud, Y., Veillard, M., 1995. Non-Stealth (poly(lactic acid/albumin)) and Stealth (poly(lactic acid-polyethylene glycol)) nanoparticles as injectable drug carriers. J. Control Release 36, 49–61.

Vila, A., Sanchez, A., Tobio, M., Calvo, P., Alonso, M.J., 2002. Design of biodegradable particles for protein delivery. J. Control Release 78, 15–24.

Vittaz, M., Bazile, D., Spenlehauer, G., Verrecchia, T., Veillard, M., Puisieux, F., Labarre, D., 1996. Effect of PEO surface density on long-circulating PLA-PEO nanoparticles which are very low complement activators. Biomaterials 17, 1575–1581.

Zambaux, M.F., Bonneaux, F., Dellacherie, E., Vigneron, C., 1999. MPEO-PLA nanoparticles: effect of MPEO content on some of their surface properties. J. Biomed. Mater. Res. 44, 109–115.